scientific reports

Check for updates

OPEN

An aftermath analysis of caving characteristics and movement of overlying strata in fully mechanized longwall gob

Chenlin Wang✉, Lihui Sun & Haoran Shen

The large-scale collapse of overlying strata in the gob directly affect the safe production of coal mines; they are also the major causes of geological disasters, such as ground cracks, surface subsidence, and ground collapse. In this paper, the movement and caved characteristics of overlying strata during coal seam excavation are studied by conducting a physical model experiment. Results show that overlying strata have different movement and caved laws during the initial, intermediate, and later mining stages. During the initial mining stage, overlying strata do not collapse, and the subsidence is extremely small. During the intermediate mining stage, overlying strata cave along the vertical direction, and caved height gradually increases. Large numbers of cavities, abscission layers, and fractures exist between caved strata. The fractured area gradually increases upward, and the subsidence increases considerably. During the later mining stage, overlying strata cave along the horizontal direction. The abscission layers between the caved strata of the central are compacted. The compacted area is surrounded by a fractured area. The compacted and fractured areas increase along the horizontal direction. The subsidence curves exhibit a horizontal variation. Overlying strata evolve from the self-equilibrium stage to the vertical collapse stage, and finally, the horizontal collapse stage. The fractured area changes from a no fractured area to a fractured area, increases vertically, and finally, increases horizontally. The subsidence curve changes from extremely small to large, and finally, changes horizontally.

Keywodrs Longwall mining, Gob, Overlying strata, Movement, Caved

Longwall mining is widely used in underground coal mining[1–3]. This automatic mining method exhibits the advantages of large coal production and high efficiency[4–6]. In China, about 95% of underground coal mines use the longwall mining method, which provides technical guarantee to the development of China's coal resources[7]. The coal production of China has become the largest in the world[8,9]. Coal accounted for 55.3% of China's total energy consumption in 2023. At present, coal is still the main energy source in China.

After coal is extracted from the underground, the original equilibrium state of the strata is changed[10–14]. The stress is redistributed, and overlying strata of coal seam are deformed and destroyed[15–18]. Overlying strata are affected by coal seam mining in different degrees, leading to varying levels of deformation and failure[19–21]. The caved, fractured, and continuous deformation zones are formed from bottom to top[22–24]. When a sufficiently wide longwall panel is mined, overlying strata can form the caved, fractured, continuous deformation, and soil zones[25].

The caved zone is dominated by broken rock, without continuity and bedding plane. A large number of voids and fractures exist between caved strata[26,27]. The fractured zone is at the upper part of the caved zone. The caved strata of the fractured zone are broken and discontinuous, and the bedding plane is separated. The fractures of caved strata are developed, and vertical fractures run through several strata[28,29]. The continuous deformation zone is at the upper part of the fractured zone, and the rock strata bend and sink. The original bedding plane is maintained between rock strata, and only a few fractures exist. The degree of deformation and failure of soil zone largely depends on the geological conditions.

The caved and fractured zones have developed fractures, which are the flow channels and storage spaces for gas and wate[30–33]. During the coal mining, accumulated gas in the gob flows into the mining panel, resulting

School of Mining and Geomatics Engineering, Hebei University of Engineering, Handan 056038, China. ✉email: wag_cheli@126.com

in the risk of gas over-limit[34–36]. If mining-induced fractures run through the aquifer, then a large amount of groundwater floods into the mining panel and roadway, causing mine water inrush[37–40]. The damage range extends to the ground surface, resulting in geological disasters, such as surface subsidence, ground cracks, and ground collapse[41]. Mine gas leaks to the ground surface through mining-induced fractures, causing the greenhouse effect[42,43]. In the previous studies, scholars have not divided the evolution process of overlying strata in the gob during coal mining into stages, and there is no clear understanding of the movement law of overlying strata in different mining stages. To realize efficient, safe, and green mining, studying the movement and caved laws of overlying strata during coal mining is urgent.

In the current study, the movement and caved laws of overlying strata during panel mining are investigated by conducting a physical model experiment. First, the caved law of overlying strata is analyzed, and the caved characteristics of overlying strata during the initial, intermediate, and later mining stages are determined. Second, the subsidence law of overlying strata is analyzed, and the movement characteristics of overlying strata during the initial, intermediate, and later mining stages are determined. Finally, the evolution model of movement and caving of overlying strata is established.

Experimental scheme

Research object

The research object is panel 3305 in coal mine no.5, Hebi, Henan Province, China. The average buried depth of Panel 3305 is 527.25 m. The strike length and dip length of panel are 442.05 m and 102.8 m, respectively. The typical geological log profile is shown in Fig. 1. The minable coal seam is the No. II1 coal seam, and its average thickness is 8.26 m. The fully mechanized longwall mining method is used in this panel. The movement and caved laws of overlying strata under single coal seam mining are studied.

In addition, the movement and caved laws of overlying strata under multi-seam mining are studied. The number of coal seams is increased in the experimental model. The No. II1 coal seam is set as 4 m, and a coal seam with a thickness of 4 m is arranged at a position of 25 m below it.

Similarity coefficient

In the physical similarity simulation experiment, the experiment model and prototype must follow the similarity criterion. The similarity ratio is mainly considered from geometric parameters, mechanical parameters and time parameters. The geometric, stress and time similarity ratio of experiment model and prototype is 1:100, 1:173 and 1:10, respectively. The similarity coefficient can determine the size of experimental model.

Similar materials

Sand, calcium carbonate, borax and gypsum are used as similar materials in the experiment model. The amount of sand is the largest, followed by gypsum and calcium carbonate. Borax is used to prevent similar materials from condensing into blocks. The rock strength can determine the ratio number of materials. The amount of materials can be calculated in accordance with the thickness of rock strata, ratio number, and size of the experiment model. The length, height, and width of the experiment model are 2500, 1300, and 200 mm, respectively. The proportion of similar materials in the experimental model is listed in Table 1.

Laying of experiment Model

In the physical similarity simulation experiment, the rock strata are laid from bottom to top. The front and rear of the model are fixed with steel plates during the experiment. Proportionally configured similar materials are poured into the model frame. The similar materials are compacted by the iron blocks. The mica sheets are sprinkled evenly on the top of compacted similar materials. After the laying of experimental model is completed, it is dried for 7 days. Finally, the steel plates of the experimental model are removed.

To monitor the subsidence, the displacement monitoring points are arranged on the model surface, as shown in Fig. 2. In the experiment model of single coal seam, the displacement monitoring points are laid seven layers, and the distance between monitoring points is 10 cm. In the experiment model of multi-seam, the displacement monitoring points are laid nine layers, and the distance between monitoring points is also 10 cm.

Coal seam excavation

The left, right and lower boundaries of the physical model are displacement constraints. The width of the protective coal pillar of a panel is 30 cm. The coal seam is excavated from the left side of the model, and the excavation step is 10 cm. The time interval of each excavation is 30 min to ensure that the overlying strata do not move. In the experiment model of multi-seam, the shallow coal seam is excavated first, followed by the deep coal seam.

The subsidence is monitored with an XTDP photogrammetric system. After each excavation, a camera is used to record the coordinates of displacement monitoring points. A tape is used to measure the range of caved strata. The data analysis software is used to read the captured photos, and calculates the subsidence.

Results and discussion

This section describes the subsidence and caved laws of overlying strata during the initial, intermediate, and later mining stages. The height, length, and area of caved strata at different excavation distances are analyzed. The caved law of overlying strata at three different stages is expounded. The morphology and fracture types of caved strata are determined.

Formation	Lithology	Thickness(m)	Geological column
Lower Shihezi Formation	Medium-grained sandstone	7.83	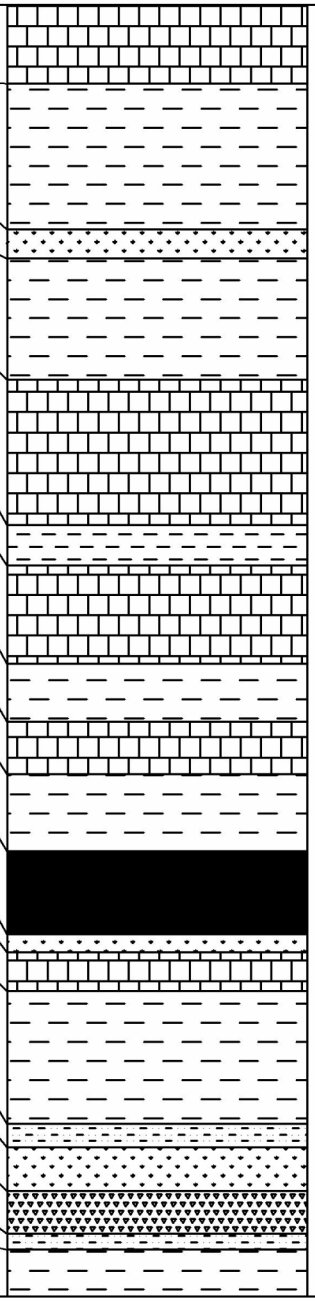
	Sandy mudstone	14.58	
	Mudstone	2.94	
	Sandy mudstone	12.12	
	Medium-grained sandstone	14.5	
Shanxi Formation	Sandy mudstone	4.06	
	Medium-grained sandstone	9.87	
	Sandy mudstone	5.78	
	Medium-grained sandstone	5.25	
	Sandy mudstone	7.71	
	II1 coal seam	8.26	
	Mudstone	1.85	
	Medium-grained sandstone	3.83	
	Sandy mudstone	13.3	
Taiyuan Formation	Fine-sandstone	2.34	
	Mudstone	4.41	
	Limestone	4.23	
	Fine-sandstone	1.61	
	Sandy mudstone	4.66	

Fig. 1. Typical geological log profile of Panel.

Initial mining stage

The movement law of overlying strata in the two experimental schemes is shown in Figs. 3 and 4. In the model experiment of single coal seam, overlying strata do not collapse before 50 cm excavation, as shown in Fig. 3. Overlying strata maintain their integrity and are in the self-equilibrium state. In the model experiment of multi-seam, overlying strata of the upper and lower gobs do not collapse before 50 cm and 40 cm excavation respectively, as shown in Fig. 4. During the initial mining stage, overlying strata do not collapse and subsidence is extremely small.

Lithology	Actual thickness /m	Actual strength /MPa	Simulated thickness /cm	Simulated strength /KPa	Proportion of similar materials	Total weight /kg	Sand /Kg	Calcium carbonate /kg	Gypsum /kg	Borax /g	Water /L
Medium-grained sandstone	7.83	20.25	7.83	117.05	355	70.61	52.96	8.83	8.83	100.87	10.09
Sandy mudstone	14.58	12.36	14.58	71.45	373	127.28	95.46	22.27	9.55	181.83	18.18
Mudstone	2.94	18.69	2.94	108.03	373	25.67	19.25	4.49	1.92	36.67	3.67
Sandy mudstone	12.12	12.36	12.12	71.45	373	105.81	79.36	18.52	7.94	151.15	15.12
Medium-grained sandstone	14.5	20.25	14.5	117.05	355	130.76	98.07	16.35	16.35	186.80	18.68
Sandy mudstone	4.06	12.36	4.06	71.45	373	35.44	26.58	6.20	2.66	50.63	5.06
Medium-grained sandstone	9.87	20.25	9.87	117.05	355	89.01	66.76	11.13	11.13	127.15	12.71
Sandy mudstone	5.78	12.36	5.78	71.45	373	50.46	37.84	8.83	3.78	72.08	7.21
Medium-grained sandstone	5.25	20.25	5.25	117.05	355	47.34	35.51	5.92	5.92	67.64	6.76
Sandy mudstone	7.71	12.36	7.71	71.45	373	67.31	50.48	11.78	5.05	96.15	9.62
II1 coal seam	8.26	5.63	8.26	32.54	573	38.66	32.21	4.51	1.93	42.95	4.30
Mudstone	1.85	18.69	1.85	108.03	373	16.15	12.11	2.83	1.21	23.07	2.31
Medium-grained sandstone	3.83	20.25	3.83	117.05	355	34.54	25.90	4.32	4.32	49.34	4.93
Sandy mudstone	13.3	12.36	13.3	71.45	373	116.11	87.08	20.32	8.71	165.87	16.59
Fine-sandstone	2.34	23.73	2.34	137.17	473	28.95	23.16	4.05	1.74	32.16	3.22
Mudstone	4.41	18.69	4.41	108.03	373	38.50	28.87	6.74	2.89	55.00	5.50
Limestone	4.23	63.56	4.23	367.40	337	58.37	43.78	4.38	10.22	83.39	8.34
Fine-sandstone	1.61	23.73	1.61	137.17	473	14.52	11.62	2.03	0.87	16.13	1.61
Sandy mudstone	4.66	12.36	4.66	71.45	373	40.68	30.51	7.12	3.05	58.12	5.81

Table 1. Proportion of similar materials in single coal seam mining.

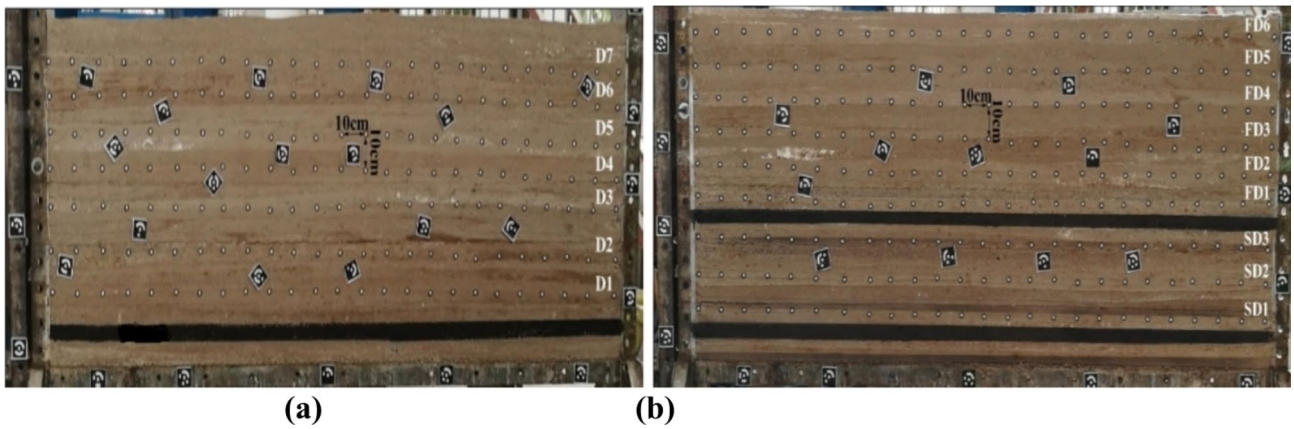

Fig. 2. The displacement monitoring points of experimental model: (**a**) single coal seam, and (**b**) multi-seam.

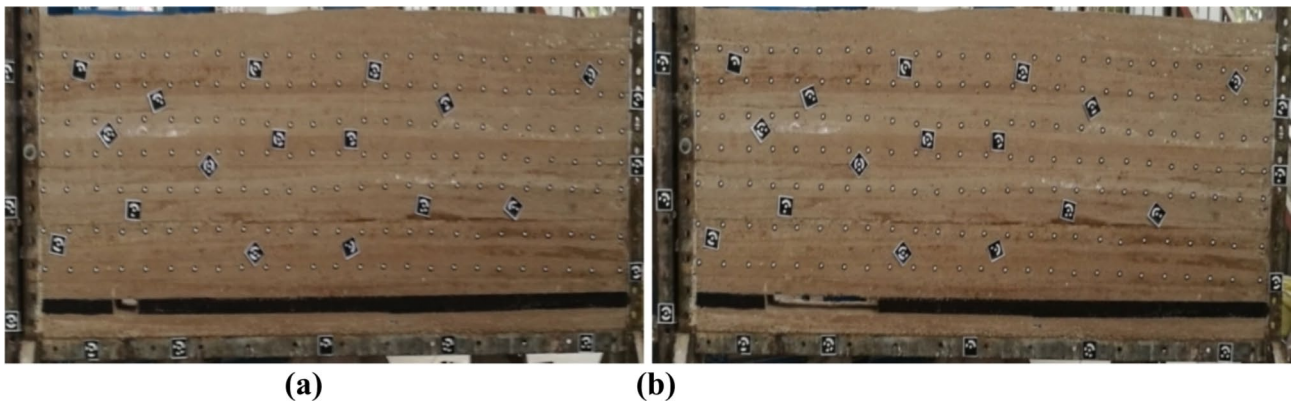

Fig. 3. The initial mining stage of single coal seam: (**a**) excavation of 10 cm, and (**b**) excavation of 50 cm.

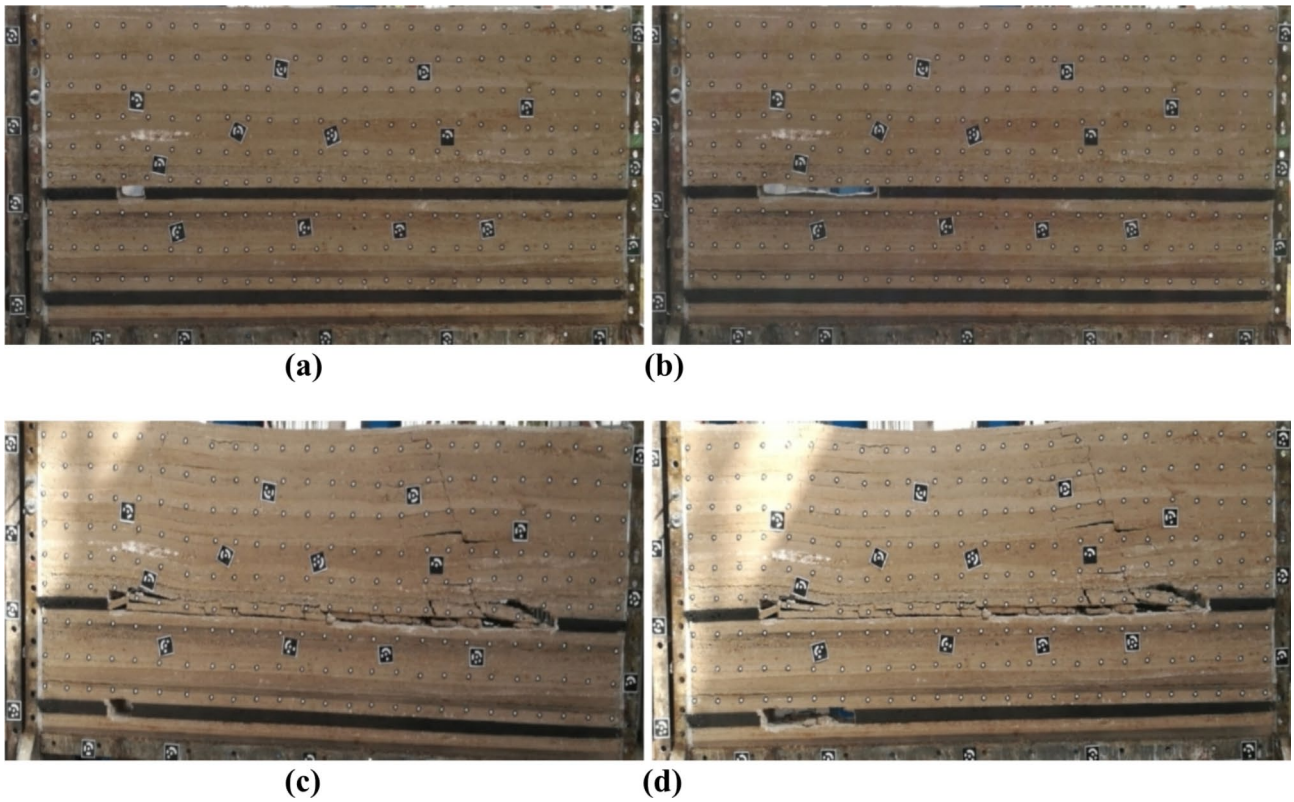

Fig. 4. The initial mining stage of multi-seam: (**a**) excavation of 10 cm in the upper gob, (**b**) excavation of 50 cm in the upper gob, (**c**) excavation of 10 cm in the lower gob, and (**d**) excavation of 40 cm in the lower gob.

The first stage is the initial mining stage. Overlying strata do not collapse, and no evident abscission layers and fractures occur. The subsidence is extremely small. Coal seam mining exerts minimal influence on overlying strata. This stage can be called the self-equilibrium stage of overlying strata.

Intermediate mining stage

This section presents the movement and caved laws of overlying strata during the intermediate mining stage. The height of caved strata at different excavation distances is calculated. The variation characteristics of the subsidence curve are analyzed.

Single coal seam

(1) Caved law

The caved law of overlying strata in the model experiment of single coal seam is illustrated in Fig. 5. When coal seam is excavated to 60 cm, the immediate roof collapses in the form of bending subsidence. The height of caved strata is 8.71 cm. When coal seam is excavated to 90 cm, the caved range extends to the lower part of the D2 survey line. The increased height of caved strata is 13.16 cm. When coal seam is excavated to 100 cm, the caved range extends to the lower part of the D4 survey line. The increased height of caved strata is 27.32 cm. When coal seam is excavated to 110 cm, the caved range extends to the lower part of the D6 survey line. The increased height of caved strata is 22.62 cm. When coal seam is excavated to 140 cm, the caved range extends to the lower part of the D7 survey line. The increased height of caved strata is 6.34 cm. The caved strata changes along the vertical direction.

(2) Movement law

The subsidence of overlying strata in the model experiment of single coal seam is shown in Fig. 6. When coal seam is excavated to 60 cm, the survey lines do not collapse, and their subsidence changes slightly. When coal seam is excavated to 140 cm, rock strata at the D6 survey line collapses and subsidence increases significantly. The lower part of the D7 survey line has an evident concave abscission layer, resulting in the small subsidence of the D7 survey line. The subsidence curves of caved strata change in the vertical direction.

Upper gob in multi-seam mining

(1) Caved law

The caved law of overlying strata is illustrated in Fig. 7. When coal seam is excavated to 60 cm, rock strata at the FD1 survey line collapses in the form of bending subsidence. The height of caved strata is 8.69 cm. When coal seam is excavated to 80 cm, the caved range extends to the lower part of the FD2 survey line. The increased height of caved strata is 2.65 cm. When coal seam is excavated to 90 cm, the caved range extends to the lower part

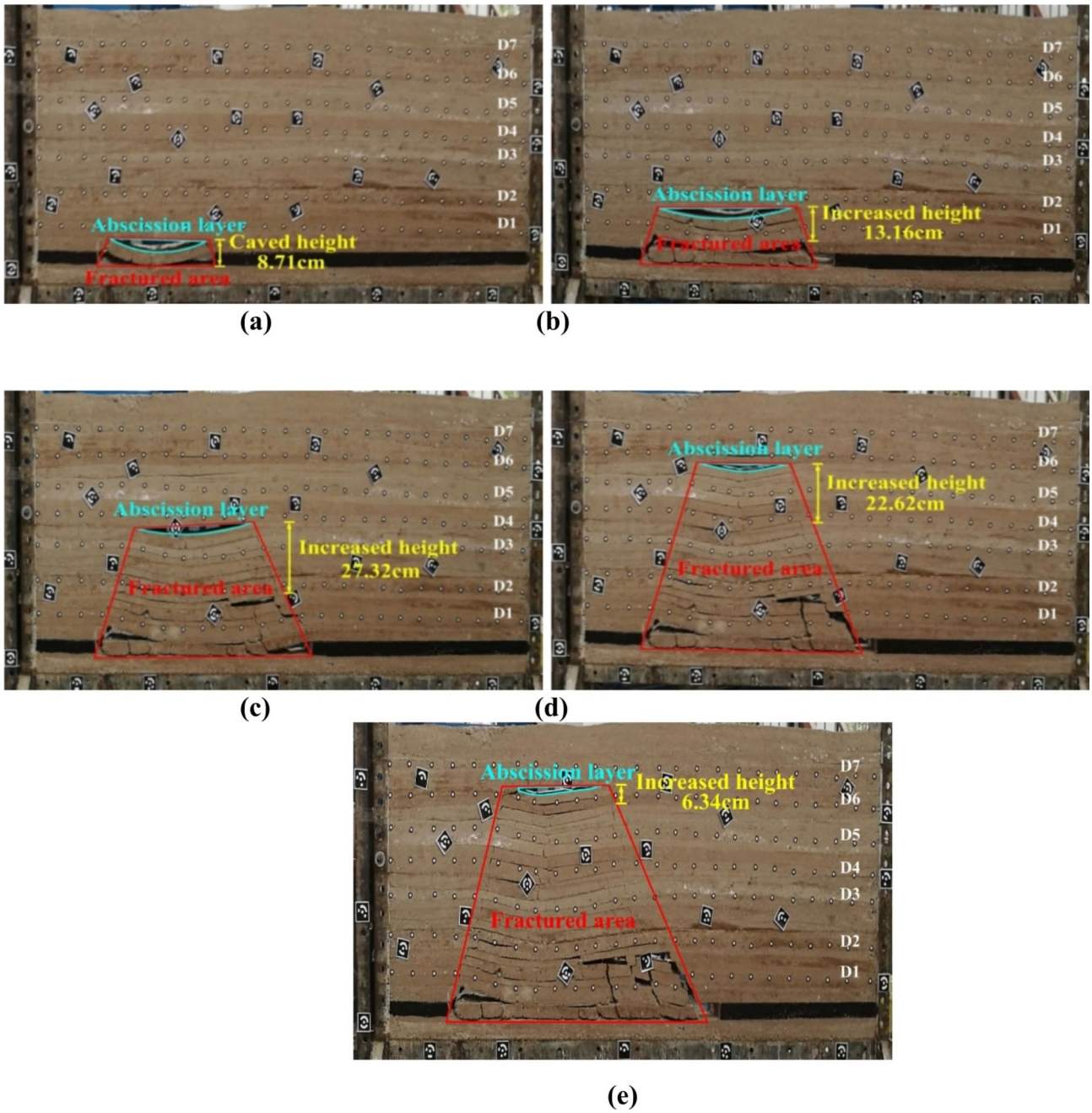

Fig. 5. Caved law-single coal seam: (**a**) excavation of 60 cm, (**b**) excavation of 90 cm, (**c**) excavation of 100 cm, (**d**) excavation of 110 cm, and (**e**) excavation of 140 cm.

of the FD4 survey line. The increased height of caved strata is 17.62 cm. When coal seam is excavated to 110 cm, the caved range extends to the lower part of the FD5 survey line. The increased height of caved strata is 11.68 cm. When coal seam is excavated to 140 cm, the caved range extends to the lower part of the FD6 survey line. The increased height of caved strata is 10.36 cm. The caved law is consistent with that of the single coal seam mining.
(2) Movement law

The subsidence curve is illustrated in Fig. 8. When coal seam is excavated to 60 cm, rock strata at the FD1 survey line collapse and the subsidence increases significantly. The subsidence curve exhibits a concave shape. When coal seam is excavated to 140 cm, rock strata at the FD5 survey line collapse and subsidence increases significantly. The lower part of the FD6 survey line has an evident concave abscission layer, resulting in the small subsidence of the FD6 survey line.

Lower gob in multi-seam mining

(1) Caved law

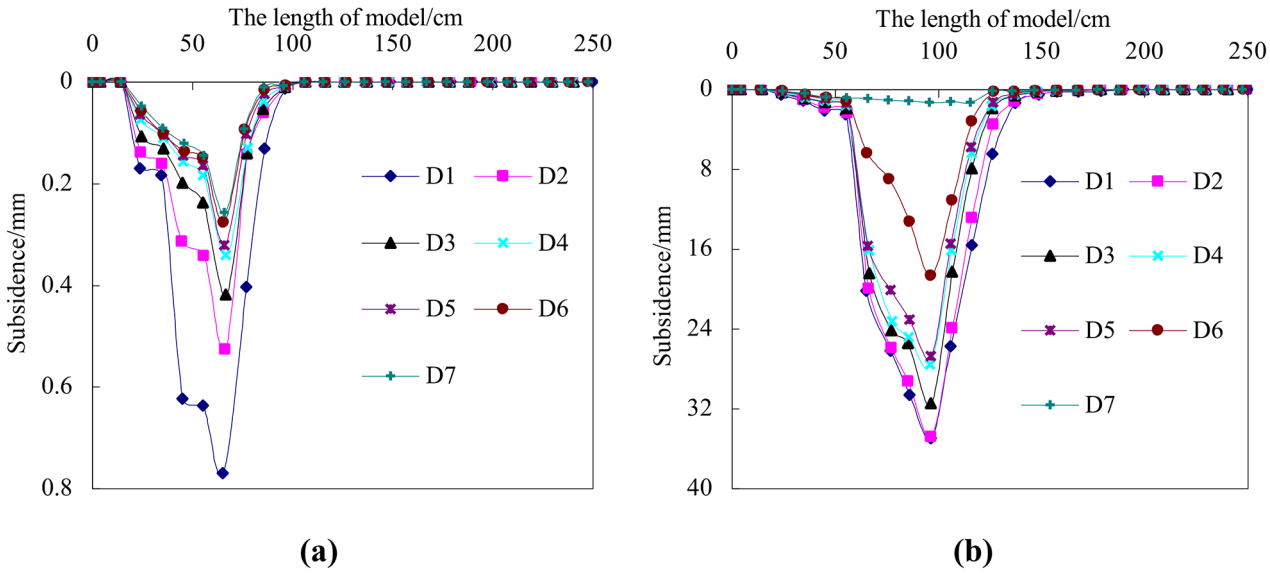

Fig. 6. Subsidence curve-single coal seam: (**a**) excavation of 60 cm, and (**b**) excavation of 140 cm.

The caved law is illustrated in Fig. 9. When coal seam is excavated to 50 cm, the lower strata of the SD1 survey line collapses. The height of the caved strata is 8.79 cm. When coal seam is excavated to 60 cm, the caved range extends to the lower part of the SD2 survey line. The increased height of caved strata is 6.21 cm. When coal seam is excavated to 90 cm, the caved range extends to the lower part of the SD3 survey line. The increased height of caved strata is 16.29 cm. The caved law is consistent with that of the single coal seam mining.

(2) Movement law

The subsidence curve is illustrated in Fig. 10. When coal seam is excavated to 50 cm, the lower strata of the SD1 survey line occurs collapse, resulting in the small subsidence of the SD1, SD2, and SD3 survey lines. When coal seam is excavated to 90 cm, rock strata at the SD2 survey line collapse and subsidence increases significantly. The lower part of the SD3 survey line has an evident concave abscission layer, resulting in the small subsidence of the SD3 survey line.

Caved and Movement models during the Intermediate Mining Stage

The second stage is the intermediate mining stage. Overlying strata collapse along the vertical direction. The height of caved strata increases gradually with the advance of the panel, as shown in Fig. 11. This stage can be called the vertical collapse stage. Large numbers of cavities, abscission layers, and fractures exist between caved strata. The fractured area is trapezoidal distribution. The subsidence curve changes in the vertical direction as shown in Fig. 12. The variation characteristics of subsidence correspond to the caved characteristics of overlying strata.

Later mining stage

This section presents the movement and caved laws of overlying strata during the later mining stage. The length of caved strata is calculated at different excavation distances. The variation characteristics of the subsidence curve are analyzed.

Single coal seam

(1) Caved law

During the later mining stage, the caved law of overlying strata is depicted in Fig. 13. When coal seam is excavated to 150 cm, the abscission layers between the caved strata of the central are compacted, forming a compacted area. The upper and lower lengths of the compacted area are 33.20 cm and 58.91 cm, respectively. The upper and lower lengths of the fractured area are 83.88 cm and 150 cm, respectively. When coal seam is excavated to 170 cm, caved strata increase along the horizontal direction. The upper and lower lengths of the compacted area are 40.01 cm and 68.35 cm, respectively. The upper and lower lengths of the fractured area are 99.83 cm and 170 cm, respectively. When coal seam is excavated to 190 cm, caved strata increase further along the horizontal direction. The upper and lower lengths of the compacted area are 68.35 cm and 102.12 cm, respectively. The upper and lower lengths of the fractured area are 126.09 cm and 190 cm, respectively. The caved strata changes along the horizontal direction.

(2) Movement law

During the later mining stage, the subsidence curve is illustrated in Fig. 14. When coal seam is excavated to 150 cm, the caved distance of the D1–D7 survey lines in the horizontal direction is 139.55, 120.13, 106.32, 99.53, 93.86, 87.49, and 68.36 cm, respectively. When coal seam is excavated to 190 cm, the caved distance of the

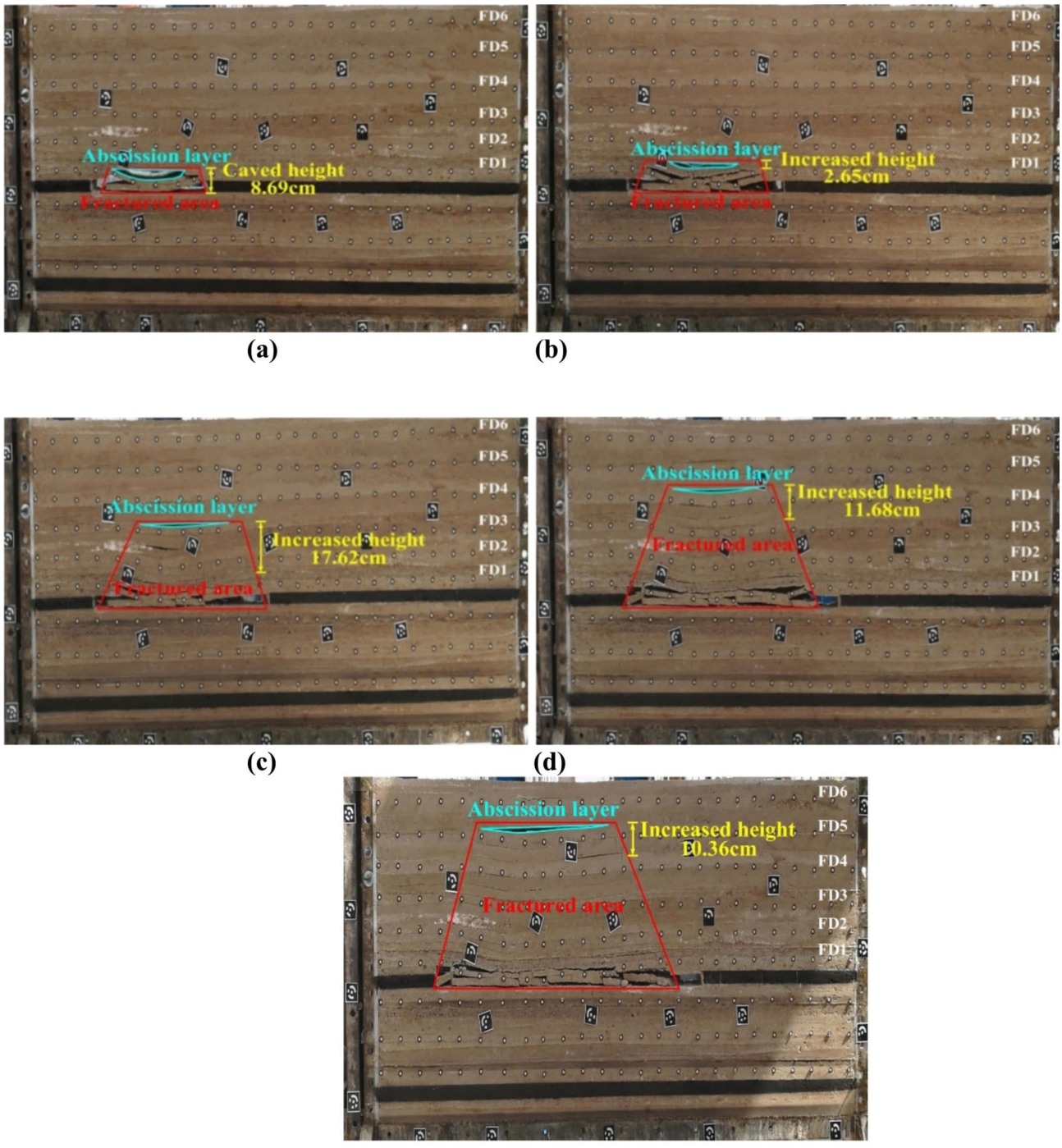

Fig. 7. Caved law-upper gob: (**a**) excavation of 60 cm, (**b**) excavation of 80 cm, (**c**) excavation of 90 cm, (**d**) excavation of 110 cm, and (**e**) excavation of 140 cm.

D1–D7 survey lines in the horizontal direction is 185.25, 168.53, 156.85, 143.77, 140.37, 128.36, and 110.33 cm, respectively. The subsidence curve changes along the horizontal direction.

Upper gob in multi-seam mining

(1) Caved law

During the later mining stage, the caved law is illustrated in Fig. 15. When coal seam is excavated to 150 cm, the abscission layers between the caved strata of the central are compacted, forming a compacted area. The upper and lower lengths of the compacted area are 43.49 cm and 68.79 cm, respectively. The upper and lower lengths of the fractured area are 92.57 cm and 148.83 cm, respectively. When coal seam is excavated to 170 cm, caved strata

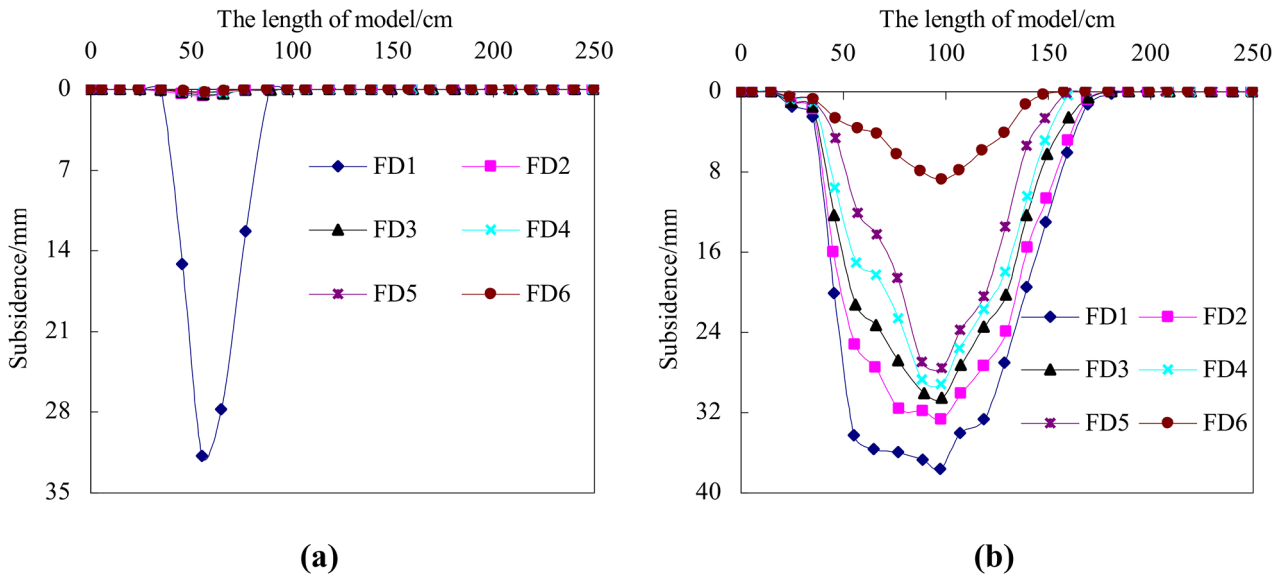

Fig. 8. Subsidence curve-upper gob: (**a**) excavation of 60 cm, and (**b**) excavation of 140 cm.

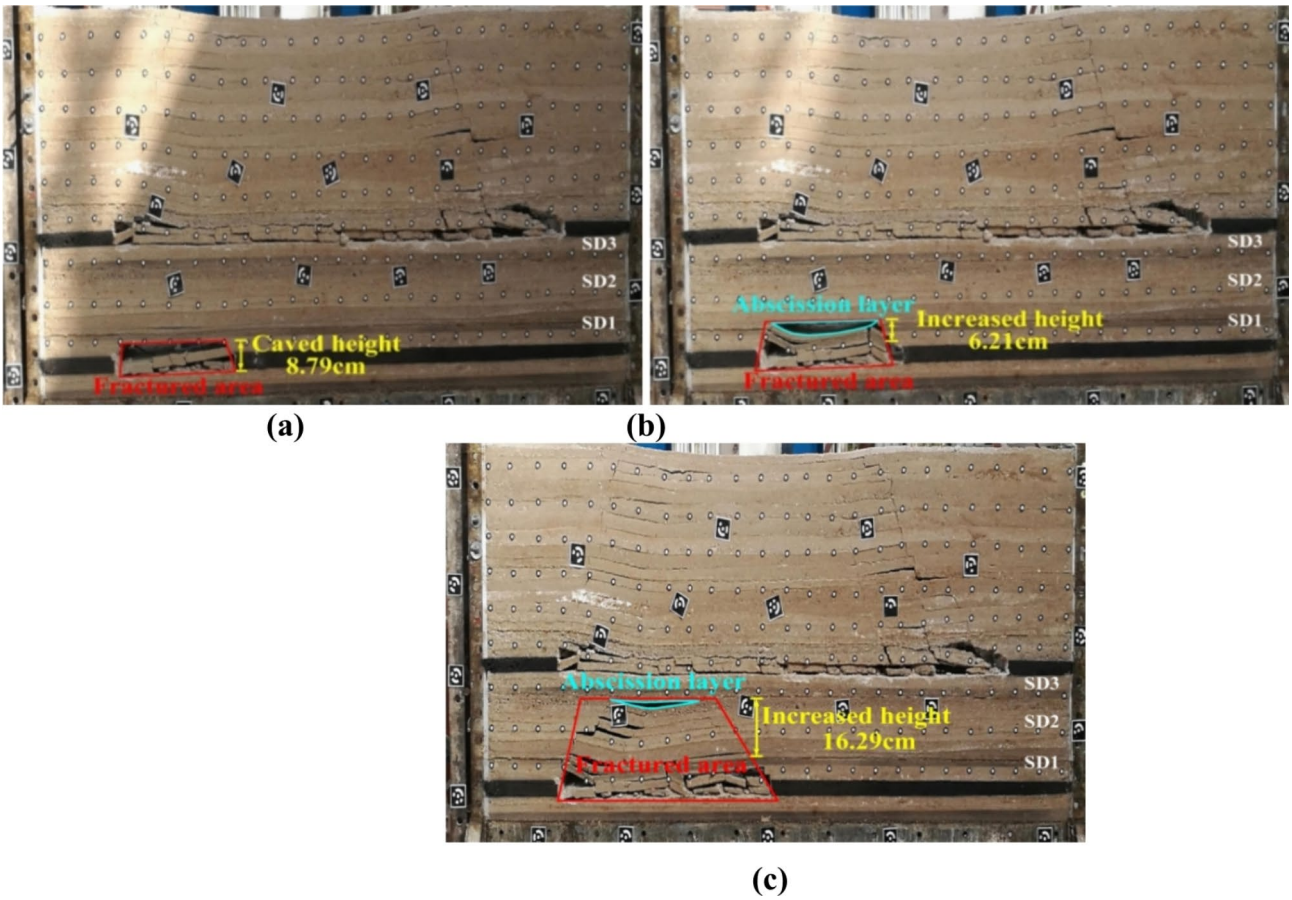

Fig. 9. Caved law-lower gob: (**a**) excavation of 50 cm, (**b**) excavation of 60 cm, and (**c**) excavation of 90 cm.

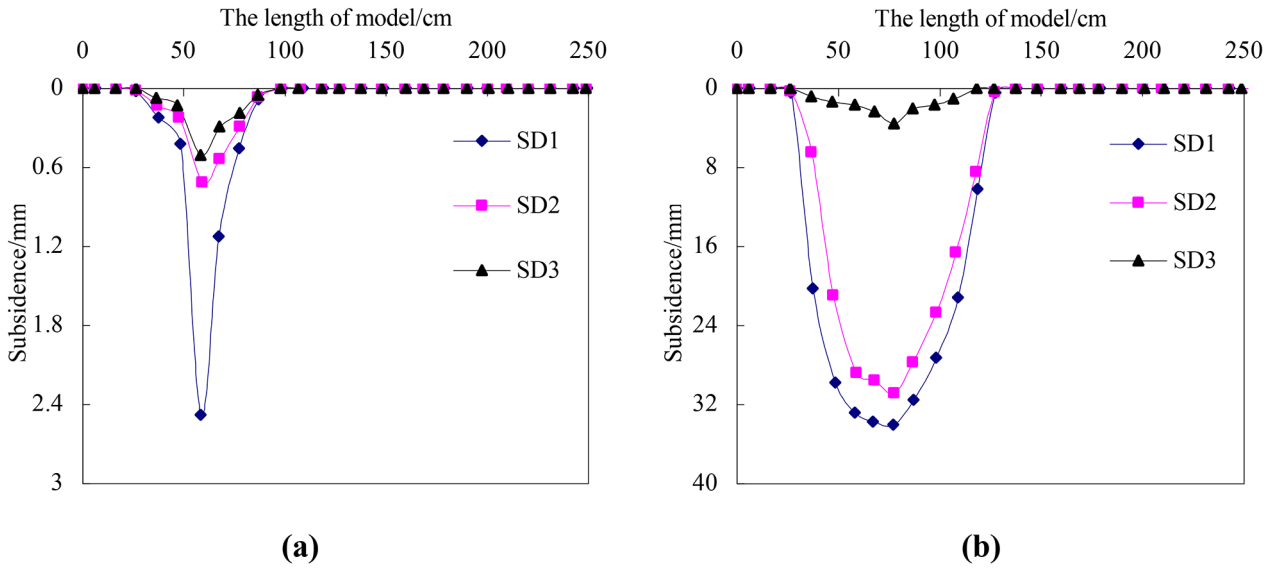

Fig. 10. Subsidence curve-lower gob: (**a**) excavation of 50 cm, and (**b**) excavation of 90 cm.

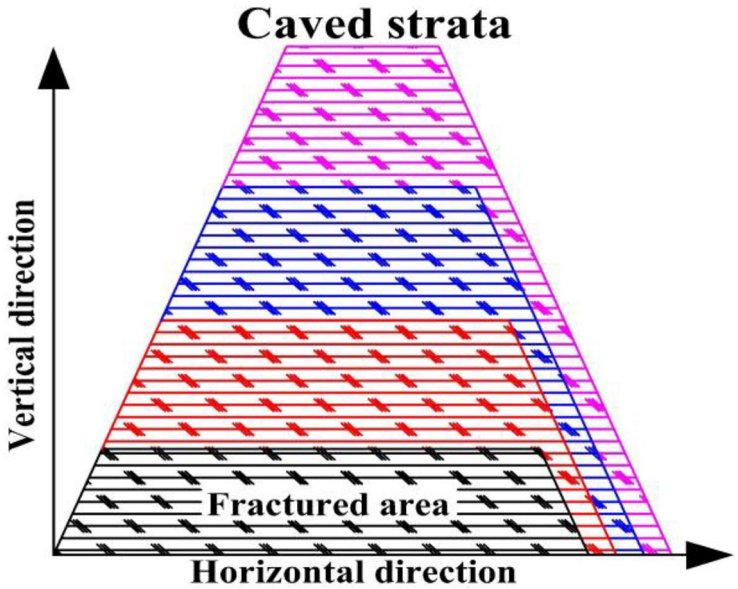

Fig. 11. Caved model-Stage II.

increase along the horizontal direction. The upper and lower lengths of the compacted area are 59.87 cm and 91.72 cm, respectively. The upper and lower lengths of the fractured area are 112.49 cm and 170 cm, respectively. When coal seam is excavated to 190 cm, caved strata increase further along the horizontal direction. The upper and lower lengths of the compacted area are 62.55 cm and 95.78 cm, respectively. The upper and lower lengths of the fractured area are 119.53 cm and 183.52 cm, respectively. The caved law is consistent with that of the later excavation stage of single coal seam.

(2) Movement law

During the later mining stage, the subsidence curve is illustrated in Fig. 16. When coal seam is excavated to 150 cm, the caved distance of the FD1, FD2, FD3, FD4, FD5, and FD6 survey lines in the horizontal direction is 132.16, 122.19, 113.52, 108.29, 92.37, and 104.31 cm, respectively. When coal seam is excavated to 190 cm, the caved distance of the FD1, FD2, FD3, FD4, FD5, and FD6 survey lines in the horizontal direction is 181.76, 165.52, 151.63, 132.34, 120.67, and 112.77 cm, respectively. The opening of the subsidence curve gradually increases with an increase in excavation distance. The variation law is consistent with that of the later mining stage of single coal seam.

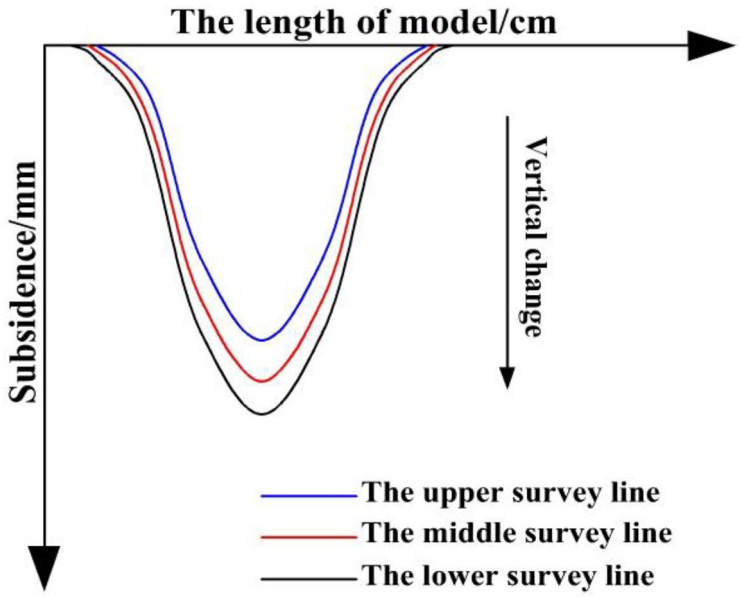

Fig. 12. Movement model-Stage II.

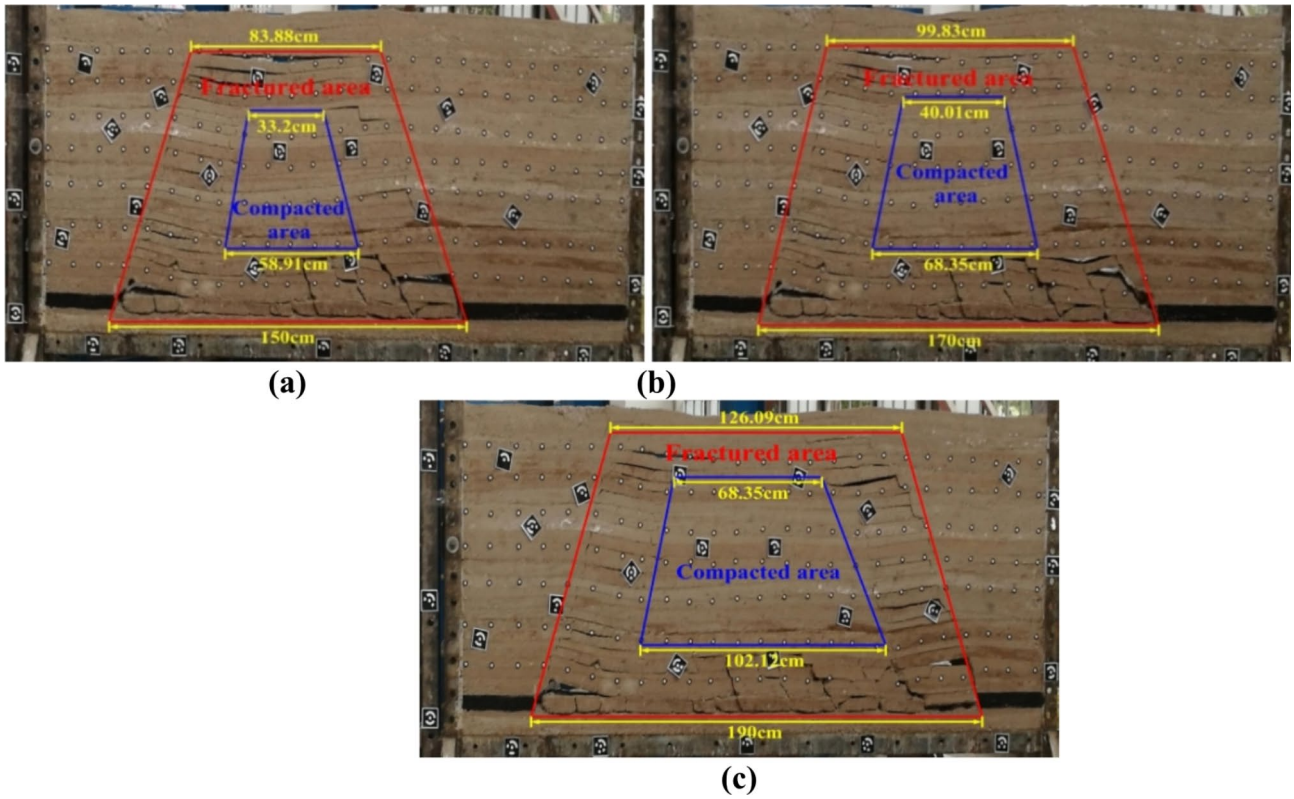

Fig. 13. Caved law-single coal seam: (**a**) excavation of 150 cm, (**b**) excavation of 170 cm, and (**c**) excavation of 190 cm.

Lower gob in multi-seam mining

(1) Caved law

During the later mining stage, the caved law is illustrated in Fig. 17. When coal seam is excavated to 100 cm, the abscission layers between the caved strata of the central are compacted, forming a compacted area. The upper boundary of the compacted area is connected to the upper gob. The upper and lower lengths of the compacted

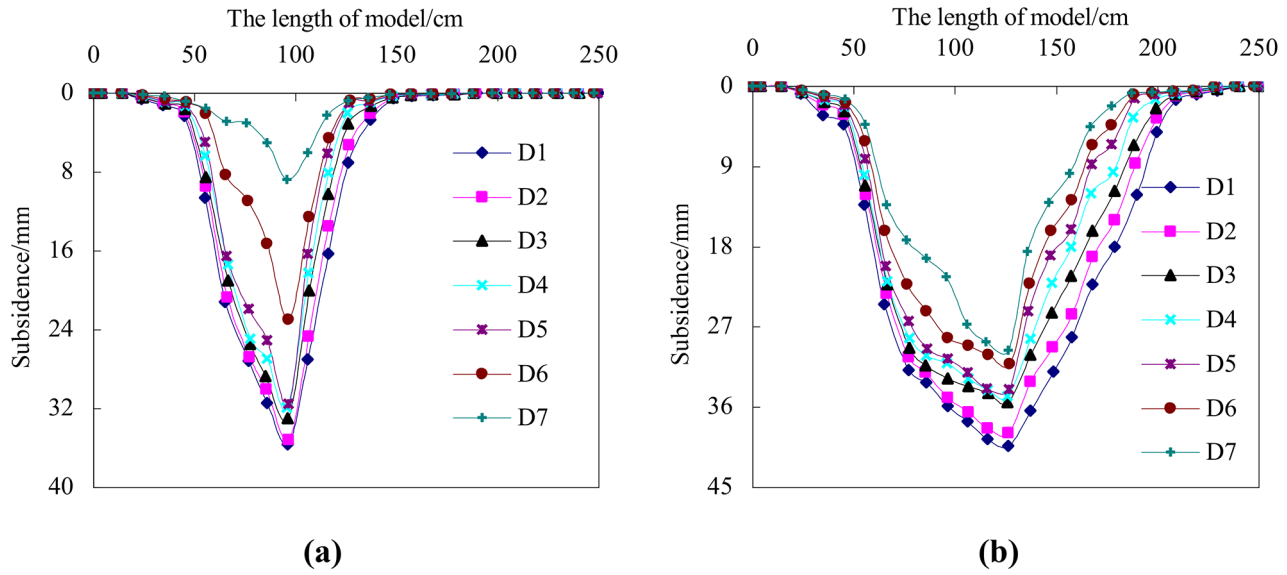

Fig. 14. Subsidence curve-single coal seam: (**a**) excavation of 150 cm, and (**b**) excavation of 190 cm.

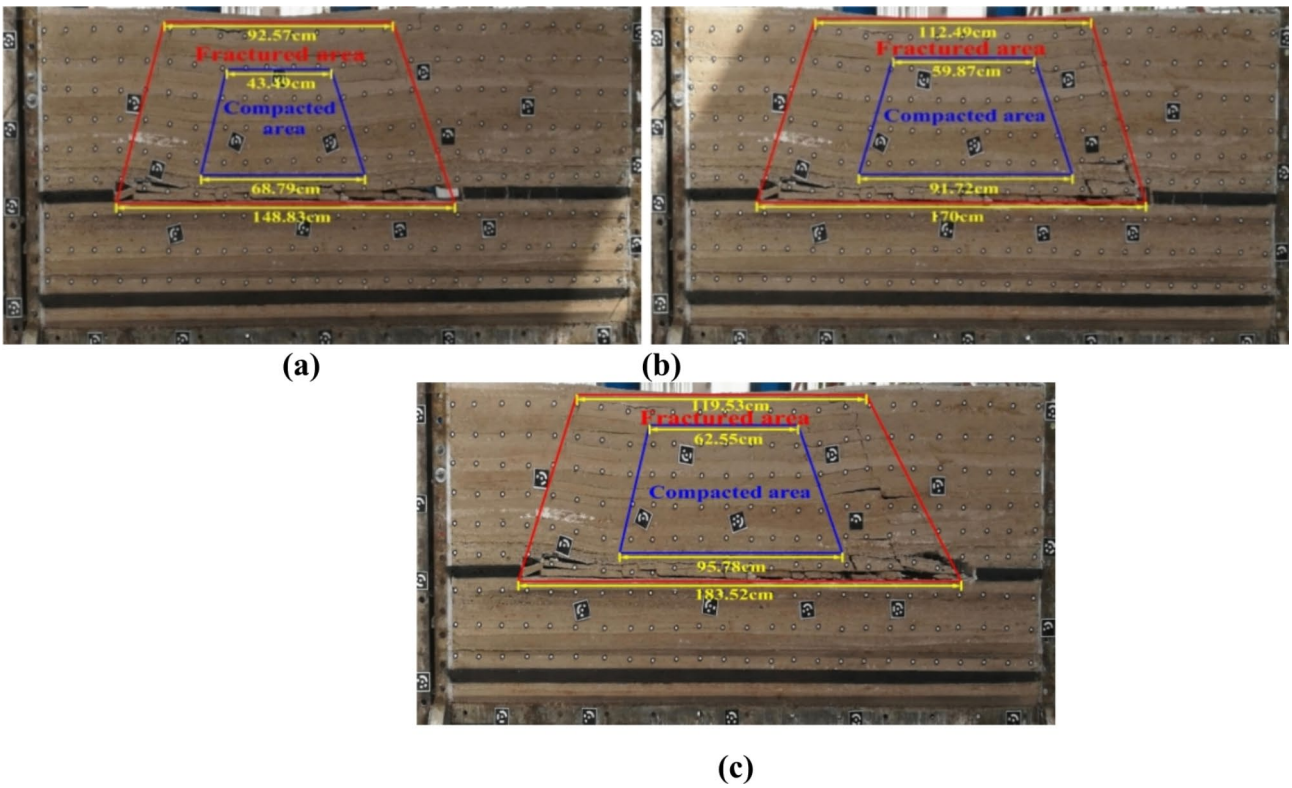

Fig. 15. Caved law-upper gob: (**a**) excavation of 150 cm, (**b**) excavation of 170 cm, and (**c**) excavation of 190 cm.

area are 18.59 cm and 40.25 cm, respectively. The upper and lower lengths of the fractured area are 46.43 cm and 100 cm, respectively. When coal seam is excavated to 150 cm, caved strata increase along the horizontal direction. The upper and lower lengths of the compacted area are 53.39 cm and 74.59 cm, respectively. The upper and lower lengths of the fractured area are 68.26 cm and 150 cm, respectively. When coal seam is excavated to 190 cm, caved strata increase further along the horizontal direction. The upper and lower lengths of the compacted area are 116.17 cm and 132.73 cm, respectively. The upper and lower lengths of the fractured area are 45.61 cm and 190 cm, respectively. The caved law is consistent with that of the later mining stage of single coal seam.

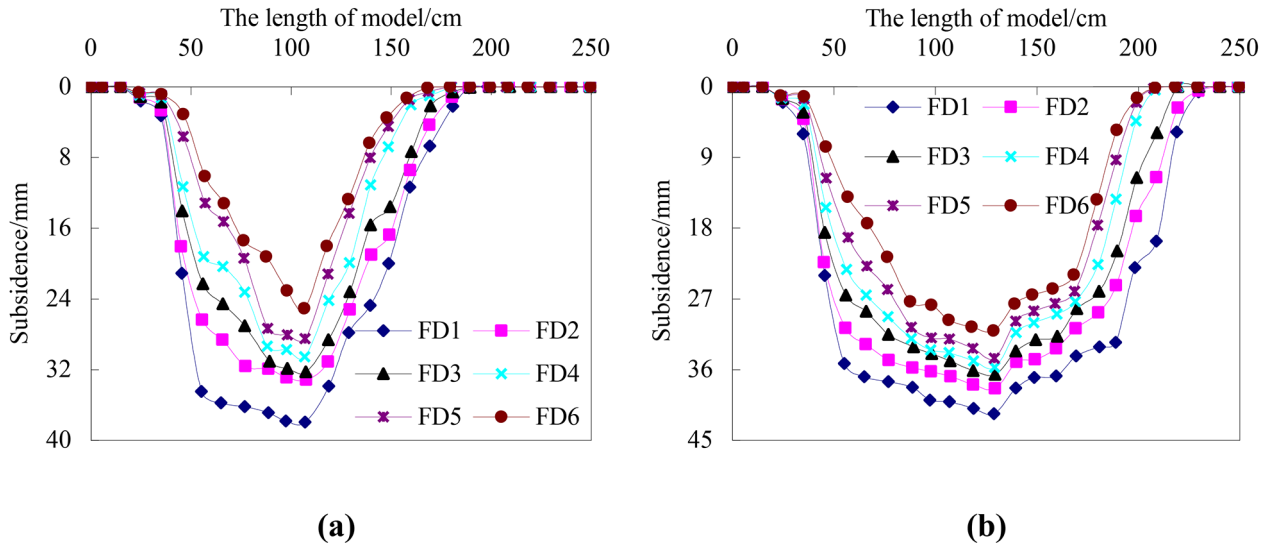

Fig. 16. Subsidence curve-upper gob: (**a**) excavation of 150 cm, and (**b**) excavation of 190 cm.

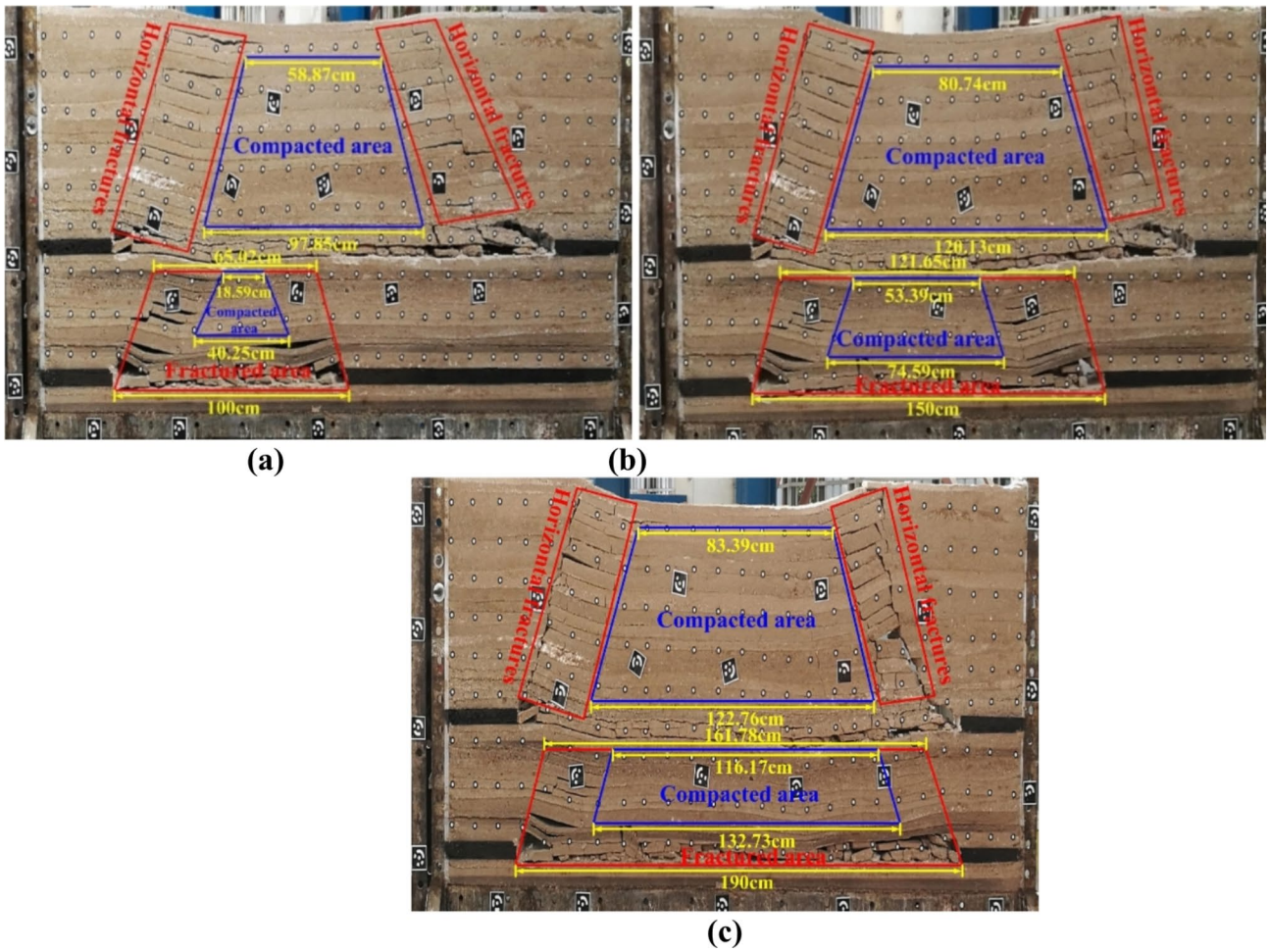

Fig. 17. Caved law-lower gob: (**a**) excavation of 100 cm, (**b**) excavation of 150 cm, and (**c**) excavation of 190 cm.

During the later mining stage, the lower gob is connected to the upper gob. The lower gob is affected by the gravity of the upper gob. The compacted area of the lower gob appears when coal seam is excavated to 100 cm. The compacted area of the upper gob appears when coal seam is excavated to 150 cm. The compacted area of the lower gob is earlier than that of the upper gob. After the upper gob is affected by the mining, the fracture development degree increases on two sides.

In addition, the compacted area in the upper gob is also change. When coal seam is excavated to 100 cm, the upper and lower lengths of the compacted area in the upper gob are 58.87 cm and 97.85 cm, respectively. When coal seam is excavated to 150 cm, the upper and lower lengths of the compacted area in the upper gob are 80.74 cm and 120.13 cm, respectively. When coal seam is excavated to 190 cm, the upper and lower lengths of the compacted area in the upper gob are 83.39 cm and 122.76 cm, respectively. The compacted area of the upper gob increases gradually.

(2) Movement law

During the later mining stage, the subsidence curve is shown in Fig. 18. When coal seam is excavated to 100 cm, the caved distance of the SD1, SD2, and SD3 survey lines in the horizontal direction is 92.31, 78.67, and 65.02 cm, respectively. When coal seam is excavated to 190 cm, the caved distance of the SD1, SD2, and SD3 survey lines in the horizontal direction is 185.27, 175.28, and 161.78 cm, respectively. This subsidence curve changes along the horizontal direction. The variation law is consistent with that of the later mining stage of single coal seams.

The subsidence changes again after the upper gob is affected by the mining, as shown in Fig. 19. When coal seam is excavated to 150 cm, the maximum subsidence of the FD1, FD2, FD3, FD4, FD5, and FD6 survey lines increases by 4.69, 4.40, 5.44, 5.38, 5.32, and 5.26 mm, respectively. When coal seam is excavated to 190 cm, the maximum subsidence of the FD1, FD2, FD3, FD4, FD5, and FD6 survey lines increases by 4.50, 4.10, 3.60, 3.56, 3.52, and 3.48 mm, respectively.

Caved and movement models during the later mining stage

The third stage is the later mining stage. The overlying strata collapse along the horizontal direction. The length of caved strata increases gradually with the advance of panel, as shown in Fig. 20. This stage can be called the horizontal collapse stage. The abscission layers between the caved strata of the central are compacted and exhibit a trapezoidal distribution. The compacted area is surrounded by a fractured area. The fractured and compacted areas increase gradually along the horizontal direction. The subsidence curve changes in the horizontal direction, as shown in Fig. 21. The variation characteristics of subsidence correspond to the caved characteristics of overlying strata.

In multi-seam mining, the upper and lower gobs interact with each other during Stage III. The lower gob is connected to the upper gob. The caved strata of the upper gob continue to change under the influence of mining. The caved strata of the upper gob move downwards, as shown in Fig. 22. The subsidence curve changes in the vertical direction, as shown in Fig. 23.

Evolution models of caved strata during coal mining

During panel mining, overlying strata undergo a dynamic evolution process. As shown in Fig. 24, the overlying strata experience the self-equilibrium stage, followed by the vertical collapse stage, and finally, the horizontal collapse stage. As shown in Fig. 25, the subsidence of overlying strata exhibits a stage of extremely small subsidence, followed by a large subsidence, and then a horizontal change occurs. The fractured area presents a

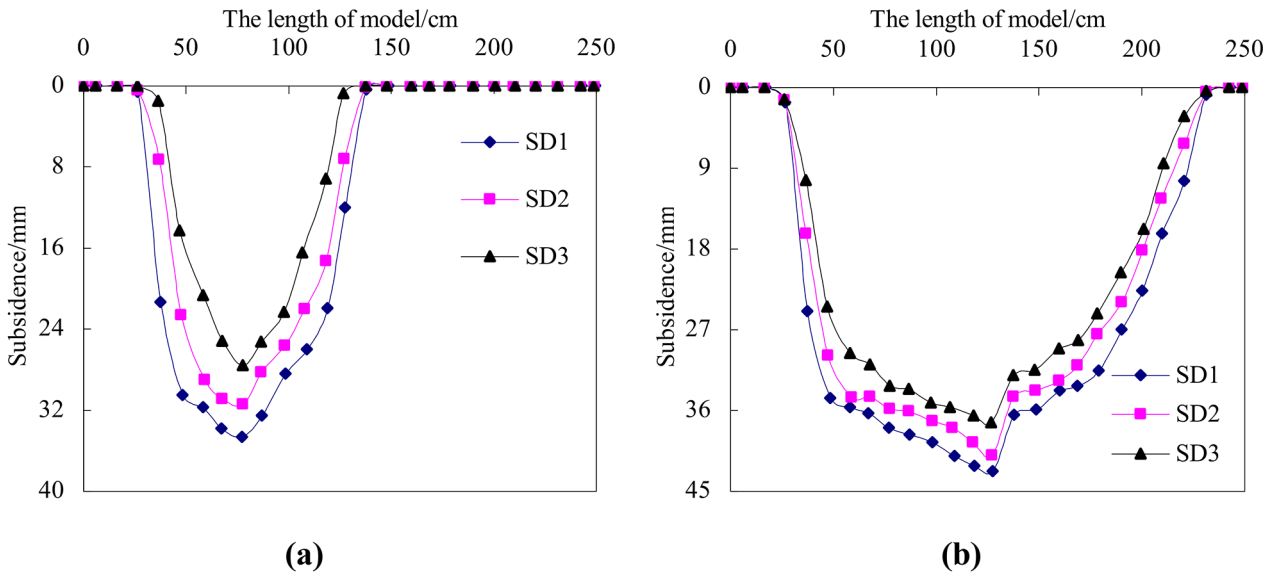

Fig. 18. Subsidence curve-lower gob: (**a**) excavation of 100 cm, and (**b**) excavation of 190 cm.

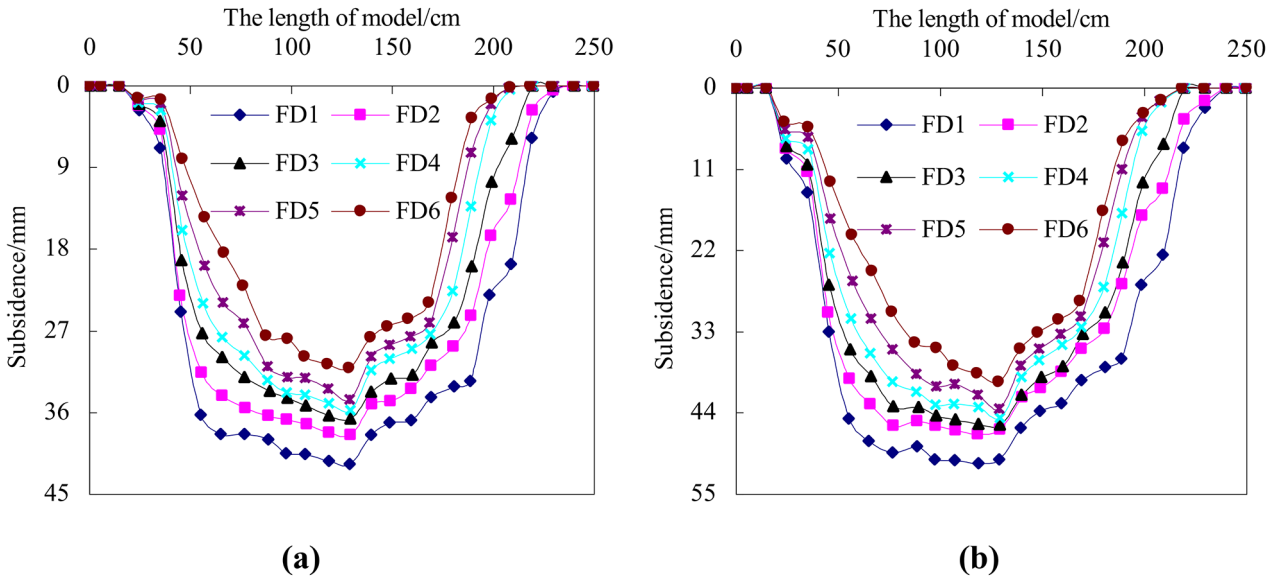

Fig. 19. Subsidence curve of the upper gob affected by the mining: (**a**) excavation of 100 cm, and (**b**) excavation of 190 cm.

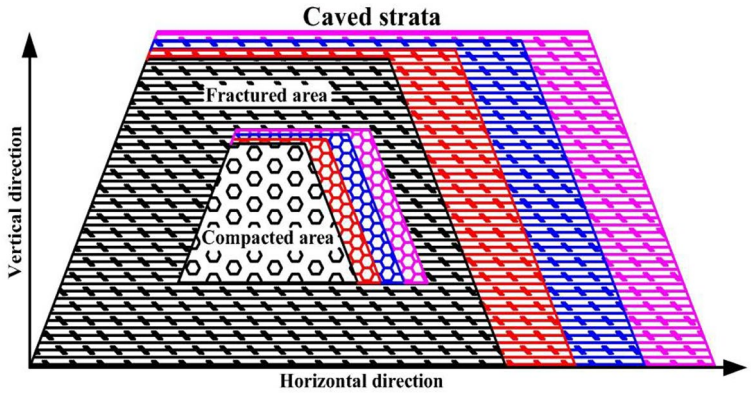

Fig. 20. Caved model-Stage III.

stage of no fractured area, followed by the vertical, and then, horizontal increase of the fractured area. During Stage III, a compacted area appears in the middle of caved strata, and increases along the horizontal direction. In addition, the lower gob is connected to the upper gob in multi-seam mining. Caved strata of the upper gob move downward again.

Conclusions

In this work, a physical similarity simulation experiment is conducted to study the movement and caved laws of overlying strata during coal seam mining. The movement characteristics of caved strata during the initial, intermediate, and later mining stages were determined. The evolution model of movement and caving of overlying strata is established. The major conclusions drawn are as follows.

(1) During the self-equilibrium stage, overlying strata in the gob do not collapse. No evident abscissions layers and fractures exist between overlying strata. The subsidence of overlying strata is extremely small. Overlying strata in the gob can realize self-equilibrium.

(2) During the vertical collapse stage, overlying strata collapse along the vertical direction, and the height of caved strata increases gradually. Large numbers of cavities, abscissions layers, and fractures exist between caved strata. The fractured area is trapezoidal distribution and gradually increases upward. The subsidence curve changes in the vertical direction.

(3) During the horizontal collapse stage, overlying strata collapse along the horizontal direction. The abscission layers between the caved strata of the central are compacted and presented a trapezoidal distribution. The compacted area is surrounded by a fractured area. The compacted and fractured areas increase along the

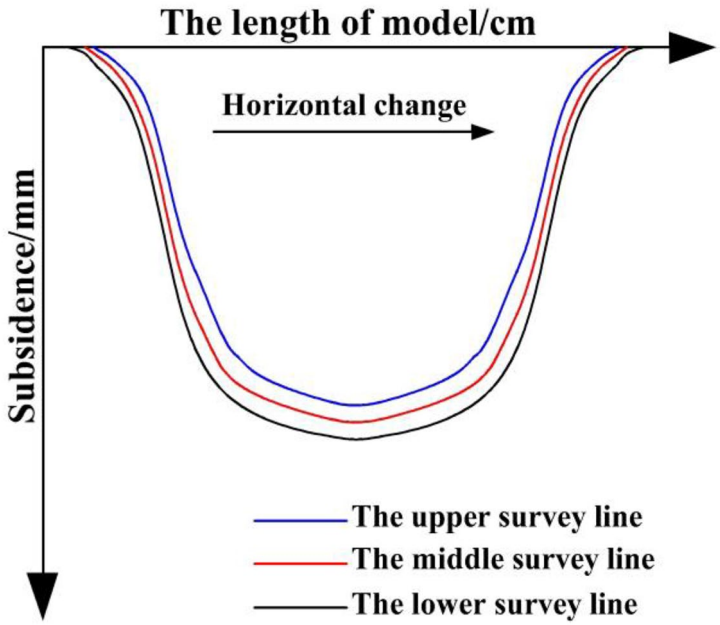

Fig. 21. Movement model-Stage III.

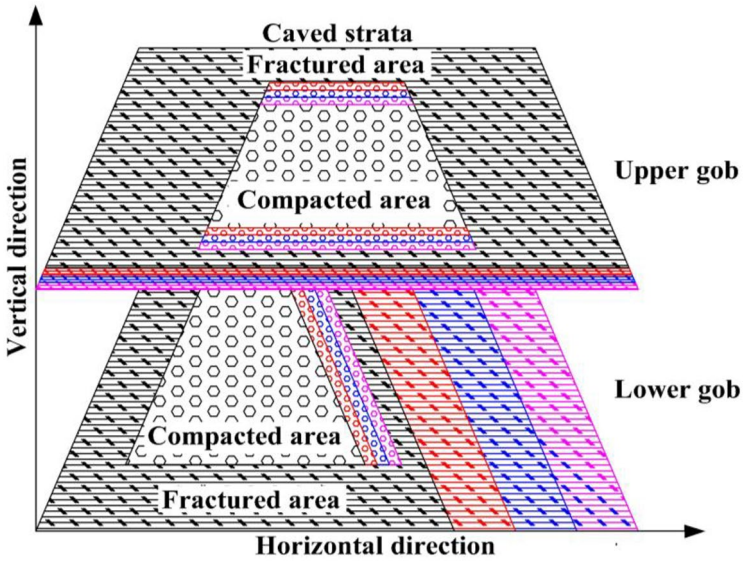

Fig. 22. Caved model-multi-seam mining.

horizontal direction. The subsidence curves change in the horizontal direction. In multi-seam mining, the caved strata of the upper gob continue to move downwards under the influence of mining of lower coal seam.
(4) During coal mining, overlying strata evolve from the self-equilibrium stage to the vertical collapse stage, and finally, the horizontal collapse stage. The fractured area of overlying strata changes from a no fractured area to a fractured area, increases vertically, and finally, increases horizontally. The subsidence curve of overlying strata changes from an extremely small subsidence to a large subsidence, and finally, changes horizontally.

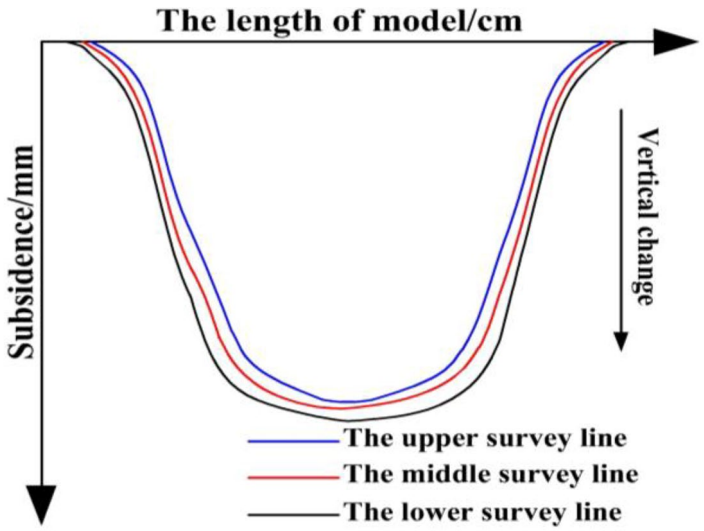

Fig. 23. Movement model-upper gob affected by the mining.

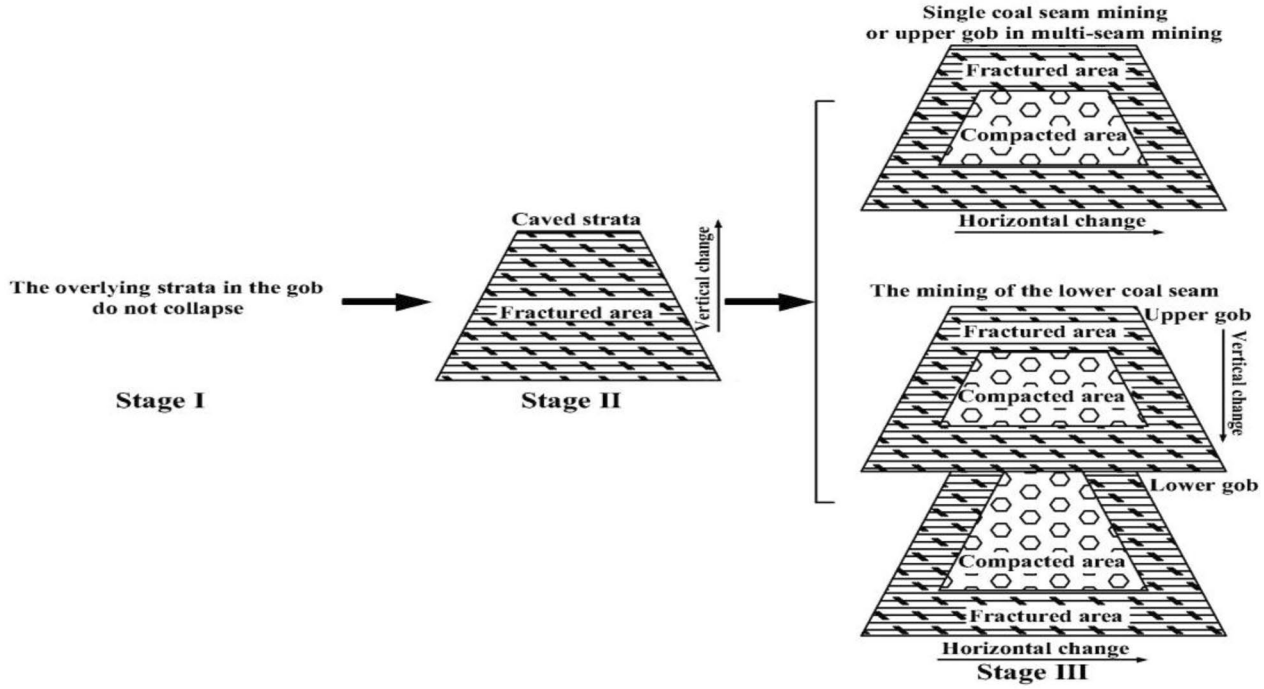

Fig. 24. Evolution model of caved strata.

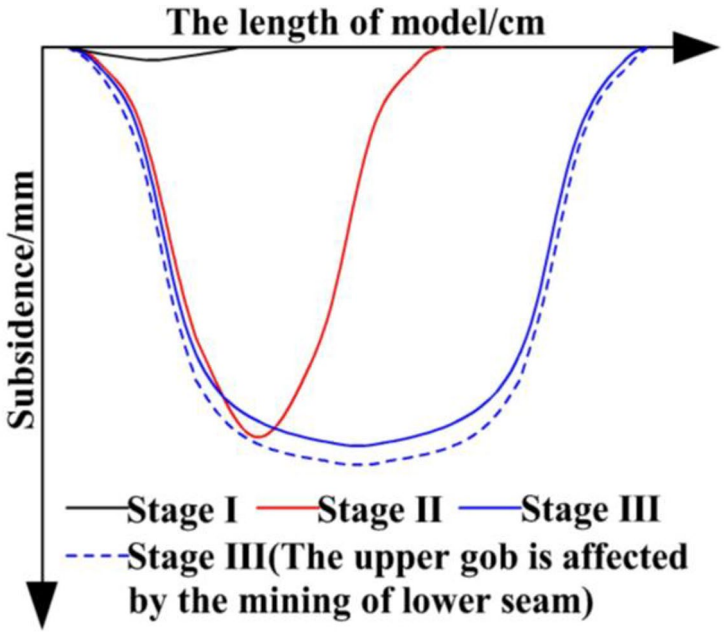

Fig. 25. Evolution model of subsidence.

Data availability

Data are available from the corresponding author on reasonable request.

Received: 29 August 2024; Accepted: 13 November 2024
Published online: 15 November 2024

References

1. Rezaei, M., Hossaini, M. F. & Majdi, A. A time-independent energy model to determine the height of distressed zone above the mined panel in longwall coal mining. *Tunn. Undergr. Space Technol.* **47**, 81–92 (2015).
2. Mangal, A. & Paul, P. S. Rock mechanical investigation of strata loading characteristics to assess caving and requirement of support resistance in a mechanized longwall face. *Int. J. Min. Sci. Techno.* **26**, 1081–1087 (2016).
3. Wang, Y. J. et al. Case study on pressure-relief mining technology without advance tunneling and coal pillars in longwall mining. *Tunn. Undergr. Space Technol.* **97**, 103236 (2020).
4. Zhang, D. S. et al. Aquifer protection during longwall mining of shallow coal seams: a case study in the Shendong Coalfield of China. *Int. J. Coal Geol.* **86**, 190–196 (2011).
5. Peng, S. S. et al. Automation in U.S. Longwall coal mining: a state-of-the-art review. *Int. J. Min. Sci. Technol.* **29**, 151–159 (2019).
6. Mahdevari, S. & Khodabakhshi, M. B. A hybrid PSO-ANFIS model for predicting unstable zones in underground roadways. *Tunn. Undergr. Space Technol.* **117**, 104167 (2021).
7. Huang, J. et al. Green and sustainable mining: Underground coal mine fully mechanized soild dense stowing-mining method. *Sustainability*. **9**, 1418 (2017).
8. Liu, H. B. & Liu, Z. L. Recycling utilization patterns of coal mining waste in China. *Resour. Conserv. Recycl.* **54**, 1331–1340 (2010).
9. Bai, X. F. et al. Coal production in China: past, present, and future projections. *Int. Geol. Rev.* **60**, 535–547 (2018).
10. Rafiqul, Islam, M., Hayashi, D. & Kamruzzaman, A. B. M. Finite element modeling of stress distributions and problems for multi-slice longwall mining in Bangladesh, with special reference to the Barapukuria coal mine. *Int. J. Coal Geol.* **78**, 91–109 (2009).
11. Xu, C. et al. Apparent-depth effects of the dynamic failure of thick hard rock strata on the underlying coal mass during underground mining. *Rock. Mech. Rock. Eng.* **52**, 1565–1576 (2019).
12. Le, T. D. & Oh, J. Longwall face stability analysis from a discontinuum-discrete Fracture Network modeling. *Tunn. Undergr. Space Technol.* **124**, 104480 (2022).
13. Wu, E. et al. Influence of different mining location on deformation characteristics of overlying strata on gently anti-dip high-steep mining slope. *Sci. Rep.* **14**, 23415 (2024).
14. Chaurasia, E. et al. Large-scale laboratory investigation of pillar-support interaction. *J. Rock Mech. Geotech. Eng.* Preprint at (2024). https://doi.org/10.1016/j.jrmge.2024.04.008
15. Yang, W. et al. Mechanism of strata deformation under protective seam and its application for relieved methane control. *Int. J. Coal Geol.* **85**, 300–306 (2011).
16. Lu, C. P. et al. Stress evolution caused by hard roof fracturing and associated multi-parameter precursors. *Tunn. Undergr. Space Technol.* **84**, 295–305 (2019).
17. Yang, Y. et al. On strata damage and stress disturbance induced by coal mining based on physical similarity simulation experiments. *Sci. Rep.* **13**, 15458 (2023).
18. Guo, L. et al. Stability evaluation of the goaf based on combination weighting and cloud model. *Adv. Civ. Eng.* 3884586 (2024). (2024).
19. Palchik, V. Localization of mining-induced horizontal fractures along rock layer interfaces in overburden: field measurements and prediction. *Environ. Geol.* **48**, 68–80 (2005).
20. Miao, X. X. et al. The height of fractured water-conducting zone in undermined rock strata. *Eng. Geol.* **120**, 32–39 (2011).
21. Mangal, A. Strata stability investigation and convergence monitoring (SSICM) in thick-seam depillaring with caving by cable bolting method. *Min. Metall. Explor.* **38**, 927–944 (2021).

22. Booth, C. J. & Spande, E. D. Potentiometric and aquifer property changes above subsiding longwall mine panels, illonois basin coalfield. *Ground Water*. **30**, 362–368 (1992).
23. Palchik, V. Formation of fractured zones in overburden due to longwall mining. *Environ. Geol.* **44**, 28–38 (2003).
24. Yavuz, H. An estimation method for cover pressure re-establishment distance and pressure distribution in the goaf of longwall coal mines. *Int. J. Rock. Mech. Min. Sci.* **41**, 193–205 (2004).
25. Gao, Y. F. Four-zone model of rockmass movement and back analysis of dynamic displacement. *J. China Coal Soc.* **21**, 51–56 (1996).
26. Palchik, V. Influence of physical characteristics of weal rock mass on height of caved zone over abandoned subsurface coal mines. *Environ. Geol.* **42**, 92–101 (2002).
27. Palchik, V. Bulking factors and extents of caved zones in weathered overburden of shallow abandoned underground workings. *Int. J. Rock. Mech. Min. Sci.* **79**, 227–240 (2015).
28. Zhang, Y. X. et al. Overburden fracture evolution laws and water-controlling technologies in mining very thick coal seam under water-rich roof. *Int. J. Rock. Mech. Min. Sci.* **23**, 693–700 (2013).
29. Cheng, G. W. et al. A zoning model for coal mining-induced strata movement based on microseismic monitoring. *Int. J. Rock. Mech. Min. Sci.* **94**, 123–138 (2017).
30. Wei, J. C. et al. Formation and height of the interconnected fractures zone after extraction of thick coal seams with overburden in western China. *Mine Water Environ.* **36**, 59–66 (2016).
31. Palchik, V. Analysis of main factors influencing the apertures of mining-induced horizontal fractures at longwall coal mining. *Geomech. Geophys. Geo-eng Geo-resour*. **6**, 37 (2020).
32. Wang, C. L. & Zhang, X. D. Fracture distribution and deformation characteristics of overlying strata in an abandoned gob under single coal seam. *SADHANA-ACAD P Eng. S.* **48**, 42 (2023).
33. Wang, M. et al. Experimental and numerical study on peak strength, coalescence and failure of rock-like materials with two folded preexisting fissures. *Theor. Appl. Fract. Mec.* **125**, 103830 (2023).
34. Wang, W. et al. Fracture failure analysis of hard-thick sandstone roof and its controlling effect on gas emission in underground ultra-thick coal extraction. *Eng. Fail. Anal.* **54**, 150–162 (2015).
35. Dursun, A. E. Statistical analysis of methane explosions in Turkey's underground coal mine and some recommendations for the prevention of these accidents:2010–2017. *Nat. Hazards*. **104**, 329–351 (2020).
36. Wang, X. & Cheng, J. Study on fissure evolution of overlying rock in lower proctective mining. *Sci. Rep.* **14**, 19206 (2024).
37. Sui, W. H. et al. Hydrogrological analysis and salvage of a deep coalmine after a groundwater inrush. *Environ. Earth Sci.* **62**, 735–749 (2011).
38. Wang, J. A. & Park, H. D. Coal mining above a confined aquifer. *Int. J. Rock. Mech. Min. Sci.* **40**, 537–551 (2012).
39. Wang, X. H. et al. Comprehensive analysis control effect of faults on the height of fractured water-conducting zone in longwall mining. *Nat. Hazards*. **108**, 2143–2165 (2021).
40. Zhu, J. et al. Overburden failure and water-sand mixture outburst conditions of weakly consolidated overlying strata in Dananhu 7 coal mine. *Sci. Rep.* **14**, 8439 (2024).
41. Yang, X. L. et al. Ground subsidence and surface cracks evolution from shallow-buried close-distance multi-seam mining: a case study in Bulianta coal mine. *Rock. Mech. Rock. Eng.* **52**, 2835–2852 (2019).
42. Saini, V., Gupta, R. P. & Arora, M. K. Environmental impact studies in coalfields in India: a case study from Jharia coal-field. *Renew. Sustainable Energy Rev.* **53**, 1222–1239 (2016).
43. Karacan, C. Ö. & Warwick, P. D. Assessment of coal mine methane (CMM) and abandoned mine methane (AMM) resource potential of longwall panels: Example from Northern Appalachian Basin, USA. *Int. J. Coal Geol.* **208**, 37–53 (2019).

Author contributions
Wang wrote the main manuscript text. Sun and Shen reviewed the manuscript.

Funding
This work was supported by the Doctoral special fund of Hebei University of Engineering (No. SJ2401002055), the key research and development project of Xingtai City (Grant No. 2022ZC064).

Declarations

Competing interests
The authors declare no competing interests.

Additional information
Correspondence and requests for materials should be addressed to C.W.